Relaxation of a single-particle excitation in a Fermi system within the diffusion approximation of kinetic theory

Sergiy V. Lukyanov* Institute for Nuclear Research, 03680 Kyiv, Ukraine (Dated: November 26, 2025)

The time evolution of the Wigner distribution function for a single-particle excitation in a Fermi system was studied within the framework of the diffusion approximation of kinetic theory by numerically solving a nonlinear diffusion equation with constant kinetic coefficients. A method was proposed to separate the dissipative processes into contributions from the relaxation of the single-particle excitation and from the relaxation of the nuclear core, with a distinct relaxation time introduced for each process. The influence of the diffusion and drift coefficients on the characteristic relaxation time scale was analyzed. It was found that the resulting relaxation times exhibit a discrepancy relative to the kinetic coefficient estimates known from previous studies.

Keywords: kinetic theory; Fermi system; diffusion approximation; single-particle excitation; relaxation time

I. INTRODUCTION

The study of relaxation processes in Fermi systems is one of the key directions in modern theoretical physics, as these processes determine the time evolution of non-stationary states, the transport properties of matter, and the mechanisms by which thermodynamic equilibrium is established. Such processes manifest themselves across a wide range of phenomena — from the thermalization of excitations in heavy-ion collisions to the kinetics of collective oscillations in nuclei and the description of dense nuclear matter in astrophysical objects.

To describe the evolution of non-stationary states, the Landau–Vlasov kinetic equation is commonly employed [1]. This approach significantly simplifies the description of the system; however, the collision integral on the right-hand side of the equation remains a complicated analytical object that requires the use of specific approximations. One of these is the so-called diffusion approximation [2], within which collisions are represented as effective diffusion and drift processes in momentum space. This approach makes it possible to study the relaxation properties of the system in a generalized way without resorting to a detailed consideration of the microscopic collision mechanism.

The evolution of a Fermi system is determined by the kinetic coefficients of diffusion and drift that appear in the diffusion equation. These coefficients govern the intensity of dissipative processes of both a collective and a single-particle nature. Knowledge of their magnitudes provides information not only about the relaxation time, but also about the equilibrium temperature of the system. For example, in [3] a schematic model was proposed to describe the equilibrium state of a finite Fermi system. It was shown that the damping time of such an excitation is determined by the kinetic coefficients of the system and is given by $\tau = 4D/v^2$, where D is the diffusion coefficient

and v is the drift coefficient. The equilibrium temperature of the system is likewise expressed through a simple relation between these coefficients: $T_{eq} = -D/v$.

In [4, 5], explicit expressions for the diffusion and drift coefficients were obtained within the low-temperature approximation. However, it was found that the assumption of small transferred momenta in particle scattering near the Fermi surface [6] is insufficient to yield physically consistent results. Previously, the approximation of an isotropic nucleon scattering probability had been considered satisfactory [6, 7]. Nevertheless, when the kinetic coefficients are calculated under this assumption, divergent values arise in the integral expressions. The problem was resolved by imposing a short-range constraint on the interparticle potential. In particular, for a Gaussian potential, convergent expressions for the kinetic coefficients were obtained, and their numerical values were computed solely from phenomenological parameters of the interparticle interaction — namely, the potential depth and its effective range [5].

As is well known, within the framework of the Fermiliquid drop model, the diffusion coefficient is related to the two-particle relaxation time $\tau_{\rm coll}$ of a collective excitation, such as the giant multipole resonances in atomic nuclei [8-11]. Calculations have shown that the typical two-particle relaxation time in a nucleus is $\tau_{\rm coll}$ ~ 10^{-23} - 10^{-22} s. In [12], a phenomenological method was proposed for evaluating the effective relaxation time of an arbitrary initial excitation as it approaches its equilibrium state. The relaxation time was defined as the area under the equivalent exponential time dependence of the mean-square deviation of the distribution function, normalized to its initial value. According to this approach, for a step-like initial distribution, the relaxation time was found to be $\tau_{eq} \sim 10^{-24}$ s. The analysis showed that the obtained relaxation time τ_{eq} is approximately one order of magnitude smaller than the expected two-particle relaxation time.

At the same time, it should be noted that the effective relaxation time mentioned above characterizes the relaxation processes in the system as a whole, i.e., it includes

^{*} lukyanov@kinr.kiev.ua

both the relaxation of the single-particle excitation and that of the background. In the present work, we attempt to separate these two contributions and study the relaxation features of each component individually. In addition, we analyze how the values of the kinetic coefficients affect the time scales of the distribution function's evolution and the effective relaxation time. This makes it possible to assess how variations in the model parameters can alter the characteristic relaxation times in Fermi systems.

II. DIFFUSION APPROXIMATION TO THE KINETIC EQUATION

Consider the Landau-Vlasov kinetic equation with the collision integral on the right-hand side

$$\frac{\partial f}{\partial t} + \hat{L}f = \operatorname{St}\{f\},\tag{1}$$

where $f \equiv f(\vec{r}, \vec{p}, t)$ is the Wigner distribution function in phase space, $\operatorname{St}\{f\}$ is the collision integral, and the operator \hat{L} is defined as

$$\hat{L} = \frac{\vec{p}}{m} \cdot \vec{\nabla}_r - \left[\vec{\nabla}_r U \right] \cdot \vec{\nabla}_p, \tag{2}$$

where m is the mass of a particle. In the general case, the single-particle potential U includes both self-consistent and external fields.

For the collision integral, we will use the expression that we obtained earlier within the diffusion approximation [4, 5]

$$\operatorname{St}\{f\} = - \vec{\nabla}_{p} \cdot \left[K_{p} f(1-f) \frac{\vec{p}}{m} + f^{2} \vec{\nabla}_{p} D_{p} \right] + \vec{\nabla}_{p}^{2} [f D_{p}].$$
(3)

Here, D_p is the second moment with respect to the momentum transfer \vec{s} in the nucleon scattering process on the Fermi surface, which defines the diffusion coefficient in momentum space

$$D_p = \frac{1}{6} \int \frac{g d\vec{s}}{(2\pi\hbar)^3} \vec{s}^2 W, \tag{4}$$

and the quantity K_p defines the drift coefficient

$$K_p = \frac{m}{p} \left[\hat{p} \cdot \vec{\nabla}_p D_p - \int \frac{\mathsf{g} d\vec{s}}{(2\pi\hbar)^3} \, \hat{p} \vec{s} \, W \right], \tag{5}$$

where

$$W \approx \frac{2g}{m^2} \frac{d\sigma}{d\Omega} (s^2) \int d\vec{p}_2 \ d\vec{p}_2' \ (1 - f_2) f_2' \ \delta \left(\vec{p}_2 - \vec{p}_2' - \vec{s} \right)$$
$$\times \delta \left(\epsilon_2 - \epsilon_2' - \vec{p} \cdot \vec{s} / m \right). \tag{6}$$

Here, g=4 is the degeneracy factor of nucleons. In expression (6), $d\sigma(s^2)/d\Omega$ is the differential cross section

for nucleon scattering, and $\epsilon_2 = p_2^2/2m$, $\epsilon_2' = p_2'^2/2m$ are the single-particle energies before and after scattering.

We consider a Fermi system that models a spherical atomic nucleus in its ground state. To describe it, we use the approximation of infinite nuclear matter. In this case, the distribution function does not depend on spatial coordinates, $f = f(\vec{p},t)$, and the action of the operator \hat{L} on the distribution function is zero, $\hat{L}f = 0$. We also assume spherical symmetry of the distribution function in momentum space, $f(\vec{p},t) = f(p,t)$. For expressions (4) and (5), we apply the approximation of constant kinetic coefficients [3–5, 13, 14], namely: $D_p = D_{p,0}$ and $K_p = K_{p,0}$.

Taking into account the above approximations for the collision integral (3), the kinetic equation (1) transforms into the following nonlinear diffusion equation:

$$\frac{\partial f}{\partial t} = -\frac{K_{p,0}}{m} \left[p(1-2f) \frac{\partial f}{\partial p} + 3f(1-f) \right]
+ D_{p,0} \left[\frac{\partial^2 f}{\partial p^2} + \frac{2}{p} \frac{\partial f}{\partial p} \right],$$
(7)

which we will solve numerically in Section IV.

In this study, the values of $D_{p,0}$ and $K_{p,0}$ are treated as model parameters and may be chosen arbitrarily. At the same time, their selection is guided by the results of previous studies, in particular [14], in which these coefficients were calculated at the Fermi surface at zero temperature: $D_p^{(0)}(p_F) \approx 3.38 \times 10^{-22} \ {\rm MeV^2 \times fm^{-2} \times s}$ and $K_p^{(0)}(p_F) \approx -2.76 \times 10^{-23} \ {\rm MeV \times fm^{-2} \times s}$. In the constant-coefficient approximation, $D_{p,0}=$

In the constant-coefficient approximation, $D_{p,0} = D_p^{(0)}(p_F)$ and $K_{p,0} = K_p^{(0)}(p_F)$, and their ratio, as is known [3, 5, 13, 15], determines the equilibrium temperature of the system:

$$T_{\rm eq} = -\frac{D_{p,0}}{K_{p,0}}. (8)$$

Using the numerical values of the kinetic coefficients given above, we obtain $T_{\rm eq} \approx 12$ MeV. This value is approximately three times higher than the equilibrium temperature reported in [3, 13]. Considering that the critical temperature of nuclear matter is $T_{\rm C}=18$ MeV [16], it is evident that the coefficients $D_p^{(0)}(p_F)$ and $K_p^{(0)}(p_F)$ require refinement.

Following [3, 13], in the subsequent calculations we will use $T_{\rm eq}=4~{\rm MeV}$ as the equilibrium temperature. Then, keeping the diffusion coefficient $D_p^{(0)}(p_F)$ unchanged, we will use a drift coefficient renormalized by a factor of three in order to satisfy relation (8): $K_{p,0}\approx 3K_p^{(0)}(p_F)$.

III. RELAXATION TIME OF SINGLE-PARTICLE EXCITATION

Consider the deviation of the distribution function from its equilibrium value:

$$\delta f(p,t) = f(p,t) - f_{eq}(p). \tag{9}$$

It is clear that at time t = 0, the distribution function corresponds to the initial state:

$$f(p, t = 0) = f_{in}(p).$$
 (10)

In the case of a single-particle excitation, the initial distribution can be represented as the sum of a step-like distribution, $f_{\text{in},0}(p)$, and an excitation, $f_{\text{in},1}(p)$, which describes the single-particle peak (see Section IV):

$$f_{\rm in}(p) = f_{\rm in,0}(p) + f_{\rm in,1}(p).$$
 (11)

Let us introduce the notation for the initial deviation from the equilibrium distribution:

$$\delta f(p, t = 0) \equiv \delta f_{\rm in}(p) = f_{\rm in}(p) - f_{\rm eq}(p). \tag{12}$$

Similarly, for the step-like distribution function, we have:

$$\delta f_{\text{in},0}(p) = f_{\text{in},0}(p) - f_{\text{eq},0}(p),$$
 (13)

where $f_{eq,0}(p)$ is the equilibrium value of the distribution function to which the step-like initial distribution $f_{in,0}(p)$ evolves. Note that $f_{eq,0}(p)$ differs from the overall equilibrium distribution $f_{eq}(p)$ due to a different value of the Fermi energy. Furthermore, it is clear that the evolution of the deviation from the equilibrium of the initial step-like distribution is described by the difference:

$$\delta f_0(p,t) = f_0(p,t) - f_{eq,0}(p).$$

Substituting equations (11) and (13) into expression (12) and performing several transformations, we obtain:

$$\delta f_{\text{in}}(p) = f_{\text{in}}(p) - f_{\text{eq}}(p)
= f_{\text{in},0}(p) + f_{\text{in},1}(p) - f_{\text{eq}}(p)
= \delta f_{\text{in},0}(p) + f_{\text{eq},0}(p) + f_{\text{in},1}(p) - f_{\text{eq}}(p)
= \delta f_{\text{in},0}(p) + f_{\text{in},1}(p) - (f_{\text{eq}}(p) - f_{\text{eq},0}(p)). (14)$$

The difference between the equilibrium functions, $f_{\rm eq}(p) - f_{\rm eq,0}(p)$, in (14) defines the contribution from the single-particle excitation, i.e., its conditional equilibrium part. Let us denote it as:

$$f_{\text{eq},1}(p) = f_{\text{eq}}(p) - f_{\text{eq},0}(p).$$
 (15)

This distribution has meaning only against the background of other equilibrium functions, and in their absence or if they are identical, it equals zero.

Taking into account (15), expression (14) can be rewritten as:

$$\delta f_{\rm in}(p) = \delta f_{\rm in,0}(p) + f_{\rm in,1}(p) - f_{\rm eq,1}(p).$$
 (16)

Similarly to (9) and (13), we can write the expression for the deviation of the single-particle excitation from its equilibrium part:

$$\delta f_{\text{in},1}(p) = f_{\text{in},1}(p) - f_{\text{eq},1}(p).$$
 (17)

Then, taking into account (17), the expression (16) takes the form:

$$\delta f_{\rm in}(p) = \delta f_{\rm in 0}(p) + \delta f_{\rm in 1}(p). \tag{18}$$

We will assume that, analogously, the time evolution of these deviations behaves in the same way:

$$\delta f(p,t) = \delta f_0(p,t) + \delta f_1(p,t). \tag{19}$$

For the sake of unifying the subsequent notation, we introduce the index t (for "total"): $\delta f(p,t) \equiv \delta f_t(p,t)$, $\delta f_{\rm in}(p) \equiv \delta f_{\rm in,t}(p)$.

Similarly to the approach used in [12], we consider the root-mean-square deviation, but this time for each deviation of the distribution function:

$$\Delta_n(t) = \sqrt{\int d\vec{p} \left[\delta f_n(p,t)\right]^2},\tag{20}$$

where n = t, 0, 1. The initial values are given by:

$$\Delta_n(0) = \sqrt{\int d\vec{p} \left[\delta f_{\text{in},n}(p)\right]^2}.$$
 (21)

Let us assume that for each n the relaxation is described by an exponential law:

$$\delta f_n(p,t) = \delta f_{\text{in},n}(p) \exp\left(-t/\tau_n\right), \tag{22}$$

where τ_t is the relaxation time of the entire system, τ_0 corresponds to the step-like distribution, and τ_1 to the single-particle excitation.

Then, substituting (22) into (20) and taking into account (21), we obtain:

$$\Delta_n(t) = \Delta_n(0) \exp\left(-t/\tau_n\right). \tag{23}$$

Integrating over time:

$$\int_0^\infty \Delta_n(t)dt = \Delta_n(0) \int_0^\infty \exp\left(-t/\tau_n\right) dt.$$
 (24)

After performing the integration, we obtain:

$$\tau_n = \frac{1}{\Delta_n(0)} \int_0^\infty \Delta_n(t) dt.$$
 (25)

Substituting (23) into (25) yields an identity; however, if $\Delta_n(t)$ is not purely exponential, expression (25) defines the corresponding effective relaxation time.

IV. NUMERICAL CALCULATIONS

The diffusion equation (7) must be supplemented with an initial condition. As this condition, we first consider a step-like distribution function

$$f(p, t = 0) = f_{in,0}(p) = \Theta(p_F^2 - p^2),$$
 (26)

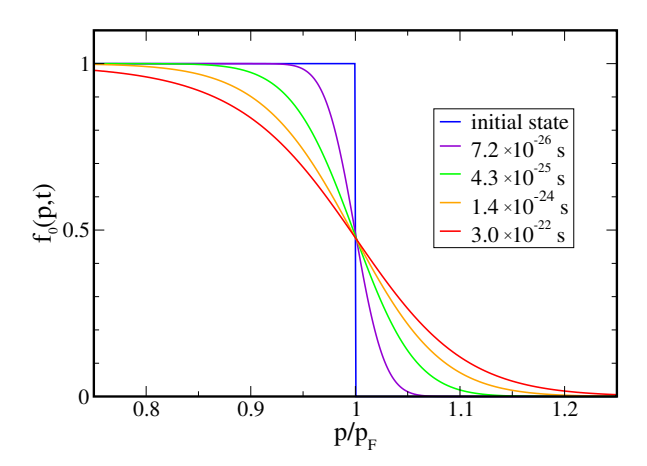


FIG. 1. (Color online) Profiles of the distribution function $f_0(p,t)$ at the time points indicated in the captions. The blue line represents the initial step-like distribution function (26), while the red curve shows the equilibrium Fermi distribution function (29), corresponding to $t = 3.0 \times 10^{-22}$ s.

where p_F is the Fermi momentum, which is determined from the condition of nucleon number conservation.

$$\frac{4\pi gV}{(2\pi\hbar)^3} \int_0^\infty dp \ p^2 f_{in,0}(p) = A. \tag{27}$$

Here, V denotes the nuclear volume. We can rewrite condition (27) in the form

$$\frac{4\pi g}{(2\pi\hbar)^3} \int_0^{p_F} dp \ p^2 = \rho, \tag{28}$$

Here, $\rho = A/V$ denotes the nuclear density. We assume that the matter density equals the standard nuclear matter density, $\rho = 0.16 \text{ fm}^{-3}$. In this case, the Fermi momentum p_F obtained from condition (28) corresponds to the Fermi energy $E_F = p_F^2/2m \approx 37.1 \text{ MeV}$.

FIG. 1 shows a set of profiles of the distribution function $f_0(p,t)$, calculated from the diffusion equation (7) at different moments in time. These profiles illustrate the overall evolution of the initial step-like distribution (26). The momentum is presented in units of the Fermi momentum p/p_F , so that $p/p_F=1$ corresponds to the Fermi surface. The figure emphasizes the region of momentum space with the highest diffusivity, approximately covering the interval $0.75 \leq p/p_F \leq 1.25$. The blue line represents the initial step-like distribution (26); the violet, green, and orange curves correspond to the profiles calculated at time points $t_1 = 7.2 \times 10^{-26}$ s, $t_2 = 4.3 \times 10^{-25}$ s, and $t_3 = 1.4 \times 10^{-24}$ s, respectively. As seen in the figure, the distribution function $f_0(p,t)$ becomes progressively smeared over time and gradually approaches the equilibrium Fermi distribution (red curve for $t \geq 3.0 \times 10^{-22}$ s).

$$f_{eq}(p) = \left(1 + \exp\left[\frac{p^2/2m - E_{F,eq}}{T_{eq}}\right]\right)^{-1},$$
 (29)

where $E_{F,eq} = 36.7$ MeV is the Fermi energy, which is lower than E_F for the step-like distribution due to the presence of the diffusive region, and is determined from the condition of nucleon number conservation:

$$\frac{4\pi gV}{(2\pi\hbar)^3} \int_0^\infty dp \ p^2 f_{eq}(p) = A.$$
 (30)

The calculation of the relaxation time according to formula (25) for n=0, based on the evolution of the distribution function shown in FIG. 1, gives the value $\tau_0 \approx 8.9 \times 10^{-24}$ s. This value is slightly larger than that obtained in [12], which results from the choice of a different, more realistic value for the nuclear matter density.

We now consider the case of a single-nucleon excitation of the nucleus, described by the following initial distribution function:

$$f_{in}(p) = \Theta(p'_F^2 - p^2) + \left[1 - \Theta(p^2 - p_2^2)\right] \Theta(p^2 - p_1^2) \Theta(p^2 - p'_F^2). (31)$$

where the particle is located beyond the Fermi surface with momentum $p_1 > p'_F$, and p'_F is the Fermi momentum determined from the nucleon number conservation condition:

$$\frac{4\pi g V}{(2\pi\hbar)^3} \int_0^{p_F'} dp \ p^2 f_{in}(p)$$

$$\equiv \frac{4\pi g V}{(2\pi\hbar)^3} \int_0^\infty dp \ p^2 f_{in,0}(p) = A - 1. \tag{32}$$

Note that the Fermi momentum p'_F is denoted with a prime to emphasize that it differs from the value p_F in the previous case of a step-like distribution in infinite nuclear matter (26). Dividing both sides of equation (32) by the nuclear volume, we obtain:

$$\frac{4\pi \mathsf{g}}{(2\pi\hbar)^3} \int_0^{p_F'} dp \ p^2 f_{in}(p) = \rho - \frac{1}{V}.$$
 (33)

where the right-hand side includes a term inversely proportional to the volume. Hence, the Fermi momentum p'_F becomes dependent on the system size.

The width of the interval in momentum space corresponding to the excited particle, $\Delta p = p_2 - p_1$, is defined by the following condition:

$$\frac{4\pi g V}{(2\pi\hbar)^3} \int_{p_F'}^{\infty} dp \ p^2 f_{\rm in}(p)$$

$$\equiv \frac{4\pi g V}{(2\pi\hbar)^3} \int_0^{\infty} dp \ p^2 f_{\rm in,1}(p) = 1, \tag{34}$$

and is inversely proportional to the mass number and to the square of the momentum (see [12], Appendix A)

$$\Delta p \approx \frac{p_F^{\prime 3}}{3Ap_1^2}.\tag{35}$$

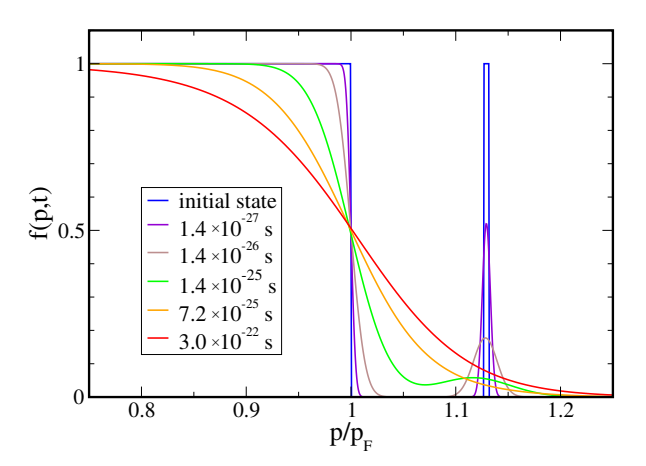


FIG. 2. (Color online) Profiles of the distribution function f(p,t) at different time moments, as indicated in the captions. The blue line corresponds to the initial distribution function (31), while the red curve represents the equilibrium Fermi distribution function (29).

According to our explanations and notations in the previous section, the distribution function (31) can be represented as the sum of two components: the first of which describes the stepwise distribution,

$$f_{\text{in},0}(p) = \Theta(p'_F^2 - p^2),$$

and the second represents the single-particle peak:

$$f_{\text{in},1}(p) = [1 - \Theta(p^2 - p_2^2)] \Theta(p^2 - p_1^2) \Theta(p^2 - {p'}_F^2).$$

FIG. 2 shows a set of profiles of the distribution function f(p,t), calculated from the diffusion equation (7) at different time moments. These profiles illustrate the overall evolution of the initial distribution (31). All notations are the same as those used in FIG. 1 As can be seen from the figure, the distribution function f(p,t), similarly to the case of the step-like distribution, gradually smooths out over time and approaches the equilibrium Fermi distribution (29) with Fermi energy $E_{F,\rm eq}'$, which is higher than the corresponding Fermi energy $E_F' = {p_F'}^2/2m$ of the initial step-like distribution. This difference arises from the one-nucleon change in the atomic number. It is also evident that, over time, the peak corresponding to the single-particle excitation gradually smooths out and eventually disappears.

Using the expression for the relaxation time (25) at n=t, we calculated its dependence on the single-nucleon excitation energy $E_{\rm ex}$ for three representative mass numbers: $A=50,\,150,\,{\rm and}\,250$. The results of these calculations are presented in FIG. 3. The blue dashed line shows the result for the step distribution in the case of infinite nuclear matter, whose profiles are presented in FIG. 1. It is evident that the relaxation time τ_0 in this case does not depend on $E_{\rm ex}$. For a finite-size Fermi system, an inverse dependence of the relaxation time $\tau_s \equiv \tau$ on the

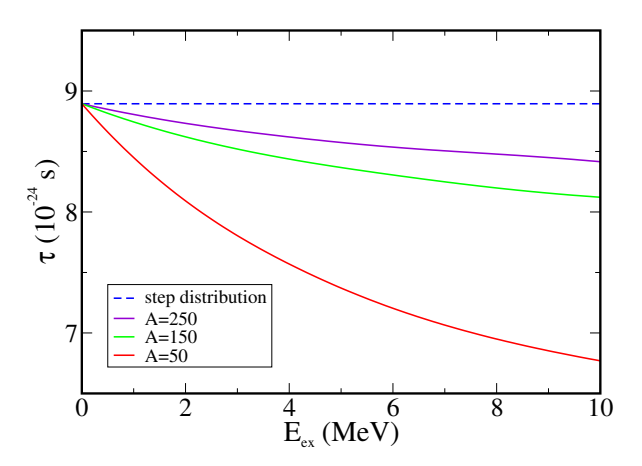


FIG. 3. (Color online) Relaxation time of the nucleus, τ , as a function of the single-nucleon excitation energy $E_{\rm ex}$. Calculations are shown for mass numbers $A=50,\,150,\,$ and 250.

excitation energy emerges. As in our previous study [12], it is seen that with increasing excitation energy, the system's relaxation time decreases nonlinearly. It is also noteworthy that as the mass number A increases, the relaxation time τ grows and approaches the limiting value for infinite nuclear matter, which is quite natural. At the same time, as in our previous work [12], the relaxation times obtained in this study are of the order of $\tau \sim 10^{-24}$ s, which is too short and does not agree with the typical two-particle relaxation time in the nucleus, $\tau_{\rm coll} \sim 10^{-23} \div 10^{-22}$ s [8–11].

Now, we study the relaxation process of a singlenucleon excitation. To this end, we separate the singleparticle excitation from the overall distribution and calculate its individual relaxation time according to formula (25) for n=1.

For a clearer understanding of the particle's behavior, FIG. 4 shows a set of profiles of the deviation of the single-nucleon distribution $\delta f_1(p,t)$, calculated using the diffusion equation (7) and constructed analogously to the previous figures. For better visibility of the details in the figure, only the lower part of the distribution, from 0 to 0.55 on the ordinate, is shown. The initial state (blue line) corresponds to the difference between the distributions $f_{\rm in}(p)$ and $f_{\rm in,0}(p)$. As seen in the figure, over time the peak of the deviation spreads out, and its maximum gradually shifts to the left—toward the Fermi surface. In the equilibrium state (red line), the nucleon is localized near the Fermi surface. In other words, it loses its initial energy and transitions to a thermodynamic equilibrium with the other nucleons of the nucleus, with the most probable momentum corresponding to the Fermi momentum. This process occurs over a characteristic time that can be described by the relaxation time τ_1 , defined according to formula (25) for n=1.

The results of this calculation are presented in FIG. 5. As seen from the figure, unlike the behavior of the overall relaxation time τ , the single-nucleon relaxation time

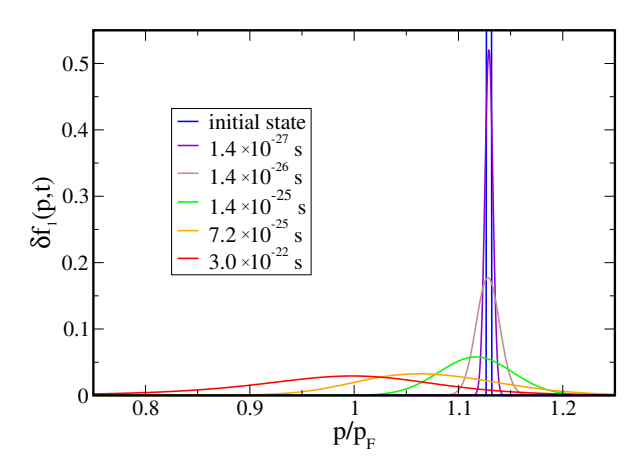


FIG. 4. (Color online) Profiles of the deviation of the distribution function $\delta f_1(p,t)$ at the time moments indicated in the captions. The blue line represents the initial difference $f_{\rm in}(p) - f_{\rm in,0}(p)$, while the red curve corresponds to the equili

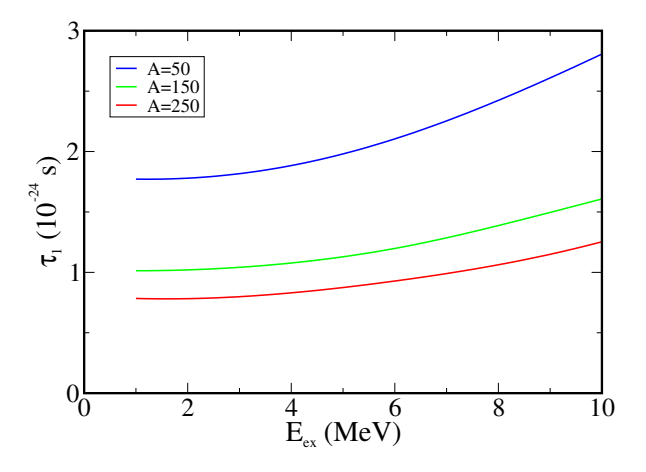


FIG. 5. (Color online) Relaxation time of a single-nucleon excitation, τ_1 , as a function of the excitation energy $E_{\rm ex}$. Calculations are shown for mass numbers A=50, 150, and 250.

 τ_1 increases with increasing excitation energy $E_{\rm ex}$. This result is quite natural, since the farther the nucleon is from the Fermi surface, the longer it takes to reach equilibrium. Moreover, the dependence on the mass number A is opposite to that of the overall relaxation time τ : as A increases, the relaxation time τ_1 decreases. This can be easily explained by noting that the width of the single-particle peak is inversely proportional to the mass number (35). That is, as A increases, the peak width decreases, and consequently, the relaxation time shortens. As observed, τ_1 is smaller than the overall relaxation time: $\tau_1 < \tau$. Hence, one can conclude that the relaxation time of an individual single-nucleon excitation is shorter than that of the nucleus as a whole. It is evident that the relaxation of the entire system occurs due to the faster single-particle processes, and therefore the

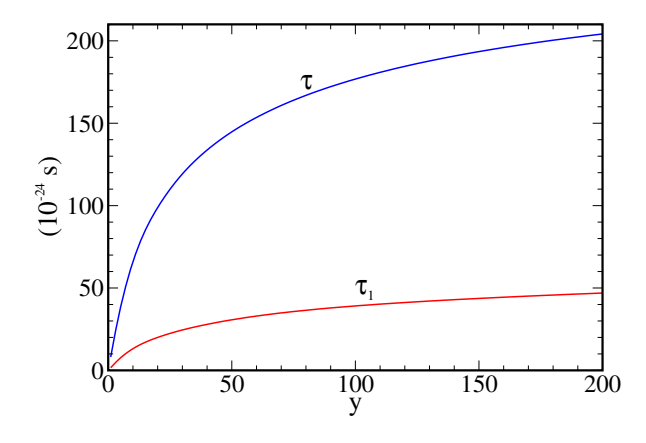


FIG. 6. (Color online) Relaxation times of the system as a whole, τ , and of the single-particle excitation, τ_1 , as functions of the parameter y.

overall relaxation time must exceed τ_1 .

Thus, the only factor that can influence the different types of relaxation times τ_n is the variation in the values of the kinetic coefficients, which determine the timescale of the evolution of the distribution function. To investigate the effect of this factor, we introduce a scaling divisor y, such that $\widetilde{D}p,0=Dp,0/y$ and $\widetilde{K}p,0=Kp,0/y$. At the same time, their ratio, which determines the system temperature, is kept constant: $D_{p,0}/K_{p,0}=\widetilde{D}p,0/\widetilde{K}p,0=-T_{\rm eq}$.

FIG. 6 shows the dependence of the overall relaxation time τ and the single-particle relaxation time τ_1 on the introduced parameter y. The calculation was performed for mass number A=150 and excitation energy $E_{\rm ex}=10$ MeV. As seen, with increasing the parameter y, both τ and τ_1 also increase. This indicates that as the diffusion and drift coefficients decrease, the relaxation rate slows down. Already with a twentyfold reduction of the kinetic coefficients, the value of τ reaches approximately 10^{-22} s. The relaxation time of the single-particle excitation, τ_1 , increases less steeply, but with a two-hundredfold reduction of the diffusion and drift coefficients, it reaches the order of 5×10^{-23} s. Thus, achieving larger relaxation times is possible only by significantly reducing the values of the diffusion and drift coefficients. However, such values contradict the estimates obtained previously [5]. Therefore, in this work, we note the presence of a discrepancy in determining the values of the diffusion and drift kinetic coefficients. Undoubtedly, this discrepancy may be influenced by the method of calculating the relaxation times; however, in our opinion, such large values of the parameter y indicate that the method itself is not the main cause of the disagreement. Clearly, the explanation should be sought in other aspects of the model.

V. CONCLUSIONS

In summary, we note that the main goal of this work was to investigate the time scales of single-particle excitation relaxation in a Fermi system, considered within the diffusion approximation of kinetic theory, in comparison with the typical two-particle relaxation time in the nucleus. For this purpose, the relaxation processes of a single-nucleon excitation in an atomic nucleus were analyzed within the diffusion approximation. The nucleus was modeled as a spherically symmetric Fermi system in both momentum and coordinate spaces. To describe the matter inside such a system, the approximation of infinite nuclear matter was employed, neglecting contributions from the system's edge. The model was described by a diffusion equation with constant kinetic diffusion and drift coefficients, whose values were chosen based on previous studies such that their ratio, determining the system's equilibrium temperature, remained physically reasonable.

The main idea of this work was to isolate the single-particle excitation from the step-like initial state of the core, against the background of which its relaxation occurs. In this context, three characteristic time scales were considered: the relaxation time of the entire system, the relaxation time of the step-like core distribution, and the relaxation time of the isolated single-particle excitation.

The calculations showed that, in all cases, the characteristic relaxation time is of the order of $\tau \sim 10^{-24}$ s, which is too short and does not agree with the typical two-particle relaxation time in the nucleus, $\tau_{\rm coll} \sim 10^{-23} \div 10^{-22}$ s [8–11]. Isolating the single-particle excitation alone demonstrated that its relaxation occurs on the same time scale as that of the system as a whole. Furthermore, the characteristic time was found to be even shorter than in the case of the step-like distribution, which is natural, since it is precisely single-particle collisions that drive the relaxation of the system's core.

The obtained dependencies of the relaxation time on

the excitation energy reveal several characteristic patterns. In particular, the relaxation time of the entire system, $\tau \equiv \tau_s$, decreases with increasing excitation energy $E_{\rm ex}$, whereas the single-particle excitation exhibits the opposite behavior, with τ_1 increasing. In both cases, the characteristic relaxation time grows with increasing mass number A; for the system as a whole, it gradually approaches the value typical for infinite nuclear matter, $\tau_0 \approx 8.9 \times 10^{-24}$ s.

It was shown that the timescale of the relaxation processes is determined solely by the values of the diffusion and drift coefficients. Varying these coefficients allows one to examine the corresponding changes in the relaxation times. To this end, a scaling divisor y was introduced, by which both coefficients were varied linearly while preserving their ratio. It was found that, as y increases, the relaxation times τ and τ_1 also increase. Hence, achieving longer relaxation times is possible only through a substantial reduction of the kinetic coefficients, although such values are inconsistent with previous estimates.

Thus, in this work, a discrepancy in the determination of the diffusion and drift coefficients has been noted. This inconsistency calls for further detailed analysis, in particular, a refinement of the assumptions underlying the diffusion approximation and an examination of the potential influence of quantum effects on the relaxation process.

ACKNOWLEDGMENTS

The author thanks the Armed Forces of Ukraine for ensuring safety during this research. Computations were performed using the supercomputing cluster of the Bogolyubov Institute for Theoretical Physics, NAS of Ukraine.

^[1] V. M. Kolomietz and S. Shlomo, *Mean Field Theory* (World Scientific, Singapore, 2020).

^[2] E. M. Lifshitz and L. P. Pitaevskii, *Physical kinetics* (Pergamon Press, Oxford, 1981) Chap. 2.

^[3] G. Wolschin, Phys. Rev. Lett. 48, 1004 (1982).

^[4] V. M. Kolomietz and S. V. Lukyanov, Ukr. J. Phys. 59, 764 (2014), arXiv:1409.1391 [nucl-th].

^[5] V. M. Kolomietz and S. V. Lukyanov, Int. Journ. Mod. Phys. E 24, 1550023 (2015), arXiv:1504.00216 [nucl-th].

^[6] A. A. Abrikosov and I. M. Khalatnikov, Rep. Progr. Phys. 22, 329 (1959).

^[7] V. M. Kolomietz, S. V. Lukyanov, V. A. Plujko, and S. Shlomo, Phys. Rev. C 58, 198 (1998), arXiv:9901048v2 [nucl-th].

^[8] G. Wegmann, Phys. Let. B 50, 327 (1974).

^[9] G. Bertsch, Z. Phys. A **289**, 103 (1978).

^[10] H. Köhler, Nucl. Phys. A 378, 181 (1982).

^[11] S. Shlomo and V. M. Kolomietz, Rep. Prog. Phys. 68, 1 (2004).

^[12] S. Lukyanov, Acta Phys. Pol. B. 56, 1 (2025), arXiv:2410.10492 [nucl-th].

^[13] T. Bartsch and G. Wolschin, Ann. Phys. 400, 21–36 (2019), arXiv:1806.04044 [cond-mat.stat-mech].

^[14] S. V. Lukyanov, Nucl. Phys. and At. Energy 24, 5 (2023), arXiv:2210.15299 [nucl-th].

^[15] S. V. Lukyanov, Int. Journ. Mod. Phys. E 30, 2150060 (2021), arXiv:2103.17129 [nucl-th].

^[16] D. Ravenhall, C. Pethick, and J. Lattimer, Nucl. Phys. A 407, 571 (1983).